Steel and Composite Structures, *Vol. 23, No. 3 (2017) 285-302*
DOI: https://doi.org/10.12989/scs.2017.23.3.285

Mitigation of seismic drift response of braced frames using short yielding-core BRBs

Muhamed Safeer Pandikkadavath and Dipti Ranjan Sahoo*

Department of Civil Engineering, Indian Institute of Technology Delhi, New Delhi-110016, India

(*Received May 03, 2016, Revised December 27, 2016, Accepted January 05, 2017*)

Abstract. Buckling-restrained braced frames (BRBFs) are commonly used as the lateral force-resisting systems in building structures in the seismic regions. The nearly-symmetric hysteretic response and the delayed brace core fracture of buckling-restrained braces (BRBs) under the axial cyclic loading provide the adequate lateral force and deformation capacity to BRBFs under the earthquake excitation. However, the smaller axial stiffness of BRBs result in the undesirable higher residual drift response of BRBFs in the post-earthquake scenario. Two alternative approaches are investigated in this study to improve the elastic axial stiffness of BRBs, namely, (i) by shortening the yielding cores of BRBs; and (ii) by reducing the BRB assemblies and adding the elastic brace segments in series. In order to obtain the limiting yielding core lengths of BRBs, a modified approach based on Coffin-Manson relationship and the higher mode compression buckling criteria has been proposed in this study. Both non-linear static and dynamic analyses are carried out to analytically evaluate the seismic response of BRBFs fitted with short-core BRBs of two medium-rise building frames. Analysis results showed that the proposed brace systems are effective in reducing the inter-story and residual drift response of braced frames without any significant change in the story shear and the displacement ductility demands.

Keywords: braced frames; buckling-restrained braces; displacement ductility; lateral load; low-cycle fatigue; seismic analysis; seismic design

1. Introduction

Concentrically braced frames (CBFs) fitted with the conventional buckling-type braces (BTBs) resist the lateral force and displacement demand under seismic loading through the axial tension yielding and compression buckling of BTBs. However, past experimental investigations have affirmed that, the local and global buckling and the low-cycle fatigue fracture characteristics of BTBs reduce the effectiveness to provide the satisfactory seismic performance of CBFs (Tang and Goel 1988, Tremblay *et al*. 2003, Celik *et al*. 2005, Fell *et al*. 2009, Kumar *et al*. 2015). Buckling-restrained braces (BRBs) are the special type of braces capable of yielding in the tension and compression axial loading without any buckling (Black *et al*. 2004). BRBs consists of a central metallic yielding core placed inside a concrete or mortar filled steel casing (Fig. 1). A de-bonding agent is provided between the central yielding core and the surrounding concrete to minimize the shear interaction between them ensuring the free expansion and contraction of yielding core under the cyclic axial loading (Watanabe *et al*. 1988). Full-scale tests on BRBs have demonstrated their ability to deliver the balanced, stable, and ductile hysteretic response with excellent low cycle fatigue capacity (Aiken *et al*. 2002, Merritt *et al*. 2003, Tsai *et al*. 2003, Tsai and Hsiao 2008, Palmer *et al*. 2014). Analytical and experimental investigations demonstrated that buckling-retrained braced frames (BRBFs) exhibit the higher drift response under the seismic loading conditions (Sabelli *et al*. 2003, Fahnestock *et al*. 2007, Erochko *et al*. 2011, Chao *et al*. 2013, Ghowsi and Sahoo 2013, 2015). This response may be primarily due to the smaller axial elastic stiffness of BRBs and the non-moment-resisting beam-to-column connections used in BRBFs. The low post-yield stiffness of BRB results in the relatively larger residual drift response of BRBFs as compared to CBFs. Several strategies have already been proposed by various researchers to control the excessive post-earthquake residual drift response of BRBFs. This includes the use of back-up moment-resisting frames (i.e., "Dual" frames) (Kiggins and Uang 2006), the incorporation of self-centering BRBs (Christopoulos *et al*. 2008, Tremblay *et al*. 2008), the use of heavier columns in BRBFs (Sahoo and Chao 2015). Though these techniques have shown the promising results, there is a need of further study on the development of simple techniques to control the drift response of BRBFs.

A BRB consists of a central core segment, two transition segments, and two end (joint) segments. The equivalent axial stiffness (K_e) of BRB can be expressed by the following equation assuming the core, transition, and end segments as elastic springs connected in series

$$K_e = EA_cA_tA_j \big/ \left(A_cA_tL_j + A_tA_jL_c + A_jA_cL_t\right) \quad (1)$$

Where, E is the Modulus of elasticity of steel; A_c, A_t, and

*Corresponding author, Ph.D.,
E-mail: drsahoo@civil.iitd.ac.in

ISSN: 1229-9367 (Print), 1598-6233 (Online)

A_j are the cross-sectional areas of core, transition and joint segments; L_c, L_t, and L_j are the lengths of core, transition and joint segments. The work point-to-work point length (L) of BRB is the algebraic sum of lengths of all three segments. For a typical BRB, the values of L_c and L_t vary in the range of 60-70% and 6-10% of the length between the work points. The values of A_t and A_j vary in the range of 1.5-2.5 times and 2.5-3.5 times the value of A_c, respectively. Using the respective values for three segments, the value of K_e can be expressed as 80-90% of elastic stiffness of core segment ($K_c = EA_c/L_c$). Thus, the elastic axial stiffness of BRBs can be increased either by increasing the area of core segments or by reducing the length of core segments.

This study is focused on the evaluation of drift response of BRBFs under seismic loading condition using the short yielding core segments of BRBs. Two different strategies have been adopted in this study incorporating the short core segments in two low-to-medium rise building frames. First strategy involves the use of BRBs of shorter length of yielding core (L_c) along with a proportionate increase in the length of end segment (L_j), referred as short yielding core length BRBs (SBRBs). Second strategy uses hybrid BRBs (HBRBs) consisting of short BRB assemblies in series with the elastic (conventional brace) segments for the remaining length (L_b) to meet the overall work point-to-work point length (L), i.e., $L = L_c + L_t + L_j + L_b$. Fig. 1 shows the schematic representation of SBRBs and HBRBs. The advantages of HBRBs are that they are less-expensive and it is easier to replace the damaged BRB assemblies in the post-earthquake scenario. The main objectives of this study are (i) to determine the limiting length of yielding core segments for BRBs; (ii) to evaluate the lateral strength, yield mechanism, and deformability of BRBFs with short core BRBs; and (iii) to compare seismic response of BRBFs with CBFs under Design-basis earthquake (DBE) and Maximum considered earthquake (MCE) hazard levels.

2. Elastic stiffness of BRBs with varying yielding core lengths

Past experimental studies have shown that SBRBs of L_c equal to $0.2L$ can withstand the displacement demands corresponding to the axial core strain of greater than 4% (Tremblay *et al*. 2006). Razavi *et al*. (2012), through analytical investigations, concluded that SBRBs are capable of accommodating the strain levels corresponding to the design story drifts. Component-level tests conducted by Pandikkadavath and Sahoo (2016a) confirmed that the SBRBs exhibit the hysteretic response and strength-adjustment factors nearly similar to those of the conventional BRBs for a minimum axial core strain of 4%. Recently, Hoveidae *et al*. (2015) have analytically shown that the use of HBRBs could reduce both inter-story and residual drift response of the braced frames. In order to account the variation of K_e due the change in yielding core length of BRBs, four different cases are considered, namely, (i) conventional BRBs without end stiffeners at the non-yielding zones (BRB1); (ii) conventional BRBs with end stiffeners at the non-yielding zones (BRB2); (iii) HBRBs without stiffeners at the non-yielding zones of BRB segments (HBRB1); and (iv) HBRBs with stiffeners at the transition and end zones of BRB segments (HBRB2). For all these cases, the value of L_t is assumed as 6% of the work point lengths (L). The cross-sectional areas of transition (A_t) and end (A_j) segments of BRBs without the end stiffeners (i.e., BRB1 and HBRB1) are considered as 1.5 and 2.0 times the BRB core area (A_c), respectively. The corresponding values for the remaining two cases with the end stiffeners (i.e., BRB2 and HBRB2) are 2.5 and 3.5 times the BRB core area (A_c). For BRB1 case, the value of L_c varied in the range of 20-80% of work-point lengths (L) and the value of L_j is adjusted proportionately. A constant value of L_j equal to $0.24L$ is used in both HBRB1 and HBRB2 cases. The elastic segment length, L_b is varied between 20-70%L in proportion to L_c, The area of elastic segments (A_b) in these cases has been assumed as $5.0A_c$.

Assuming the various segments of braces as springs connected in series, K_e can be written as follows

$$1/K_e = \sum 1/K_i \tag{2}$$

Where, K_i is the spring stiffness representing the central yielding core, transition zones, end segments of BRBs, and elastic BTB segment. Fig. 2(a) shows the variation of K_e with the change of L_c. For BRB2 case with L_c as $0.7L$, the value of K_e is found to be $1.27EA_c/L$. If the value of L_c is reduced to $0.4L$, the value of K_e is increased to $1.73EA_c/L$ indicating an increase of 36% in the axial elastic stiffness value. In case of HBRB2, the value of K_e is computed as $1.81EA_c/L$ for the same value of L_c. The increase in K_e is found to be 42.5% for the case HBRB2 with $L_c = 0.4L$ as compared to the case BRB1 with $L_c = 0.7L$. Thus, it is observed that the axial elastic stiffness of BRBs can be increased due to (i) the higher cross-sectional area at the non-yielding segments; and (ii) the smaller lengths of yielding core segments.

3. Limiting yielding core length criteria for BRBs

Though a reduction in the yielding core segments of a BRB increases its axial elastic stiffness, the displacement ductility is reduced proportionately since the maximum axial displacement is limited by the maximum axial core strain (in the range of 4-5%). This leads to the smaller energy dissipation capacity prior to the brace fracture under the cyclic loading. Therefore, there is a need to evaluate the limiting lengths of yielding core segments for SBRBs/ HBRBs to maintain a balance between the increase in the axial stiffness and the reduction in the displacement ductility capacity. The minimum yielding core length required for the acceptable non-linear performance of BRBs depends on several parameters, such as, low-cycle fatigue, maximum displacement ductility (μ_{mxm}), and cumulative displacement ductility (μ_{cum}) demands, type of loading, amplitude and number of loading cycles, material properties, and geometric properties of core segments. Ductility demands of BRBs can be defined as follows.

$$\mu_{mxm} = D_{mxm}/D_{by} \tag{3}$$

$$\mu_{cum} = \sum D_{plastic} / D_{by} \quad (4)$$

Where, D_{mxm} = maximum BRB deformation beyond yield displacement, D_{by} = BRB yield deformation, $D_{plastic}$ = BRB plastic deformation ($D_{mxm} - D_y$). The qualifying cyclic test guidelines as per ANSI/AISC 341-10 (2010) require that the BRBs should possess a maximum ductility demand corresponding to a design story drift of 2% ($D_{bm} = 4D_{by}$) and a cumulative ductility demand of 200. Assuming all other parameters are sufficient, the low-cycle fatigue fracture capacity of SBRBs primarily depends on the loading type. The minimum length of yielding core segments for a target axial strain demand in BRBs can be derived using Coffin-Manson relationship as discussed in the following sections.

Total strain capacity/demand (ε_t) is the algebraic sum of plastic strain (ε_p) and elastic strain (ε_e). Neglecting the elastic strain term, the value of ε_t can be related to the number fatigue cycles (N_f) using Coffin-Manson relationship as follows

$$\varepsilon_t = \varepsilon_p = K_p \left(N_f\right)^{-C_p} \quad (5)$$

where, K_p and C_p are the material constants and can be assumed as 0.21 and 0.485 respectively (Uriz 2005, Usami *et al*. 2011, Mirtaheri *et al*. 2011). A parameter, termed as damage index (*DI*), based on miner cycle counting law (Fisher *et al*. 1997) has been defined as follows to consider the effects of different cyclic amplitudes in the event of seismic loading.

$$DI = \sum N_i / N_{fi} \le 1 \quad (6)$$

Where, N_i = number of displacement strain amplitudes in i^{th} cycle, N_{fi} = number of cycles required to cause failure at the same strain amplitude. To avoid fatigue failure, the value of *DI* should be less than unity. ANSI/AISC 341-10 (2010) standard loading protocol for the seismic quantification tests on BRBs consisted of (i) 2 cycles of $1.0D_{by}$; (ii) 2 cycles of $0.5D_{bm}$ ($2.0D_{by}$); (iii) 2 cycles of $1.0D_{bm}$ ($4.0D_{by}$); (iv) 2 cycles of $1.5D_{bm}$ ($6.0D_{by}$); (v) 2 cycles of $2.0D_{bm}$ ($8.0D_{by}$); and (vi) 4 cycles of $1.5D_{bm}$ ($6.0D_{by}$). D_{bm} is the brace displacement corresponding to 1% of story drift and is taken as $4.0D_{by}$. Using the value of ε_t as the ratio of twice of displacement amplitudes at a particular level to the yielding core lengths of BRBs, Eq. (6) can be rewritten for this standard loading protocol as follows

$$DI = \gamma \left(2D_{by} / L_c K_p \right)^{1/C_p} \le 1 \quad (7)$$

Where, $\gamma = 2 + 2(2)^{1/C_p} + 2(4)^{1/C_p} + 6(6)^{1/C_p} + 2(8)^{1/C_p}$. Eq. (7) can be simplified to compute the minimum yielding core lengths for BRBs based on low-cycle fatigue criteria as follows

$$L_c \ge \left(2\gamma^{C_p} / K_p \right) D_{by} \quad (8)$$

In addition to the minimum yielding core lengths of BRBs based on the low-fatigue criteria, the higher mode compression buckling approach should also be checked. Since the yielding strengths of BRBs in tension and compression are nearly equal, the higher mode buckling number (n) can be computed by equating the tension

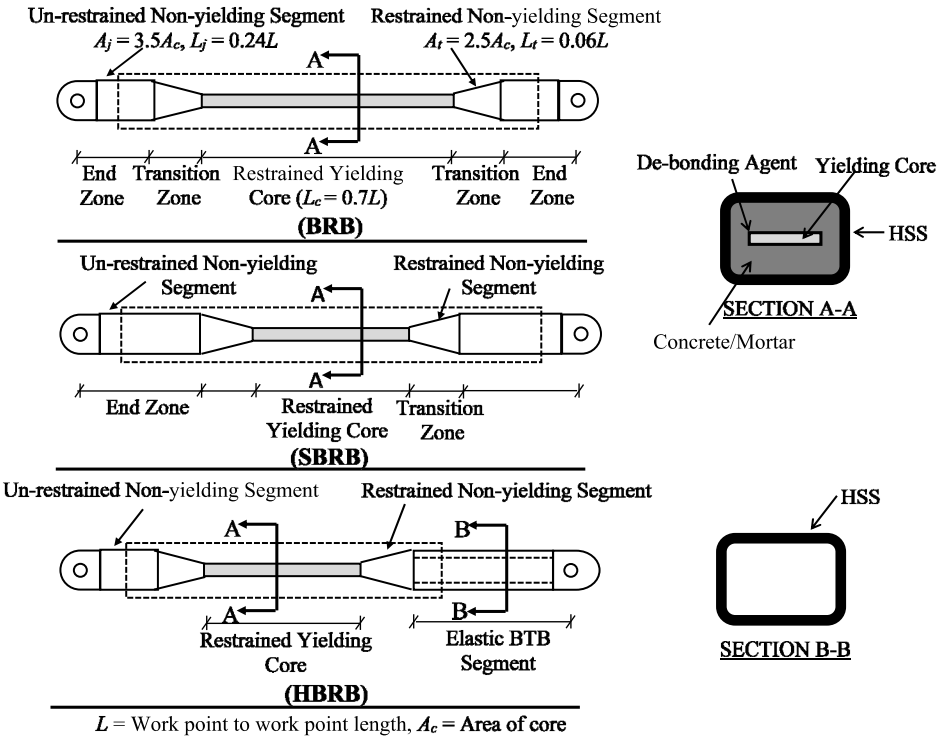

Fig. 1 Schematic representations of BRB, SBRB, and HBRB sections

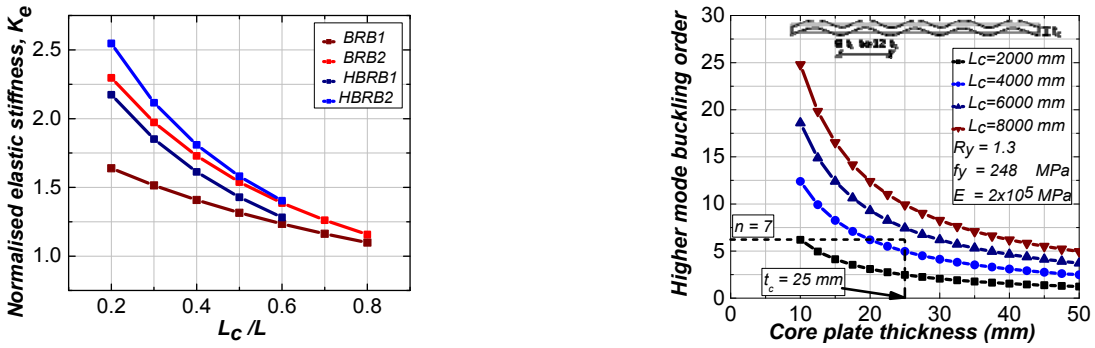

(a) (b)

Fig. 2 Variation of (a) normalized elastic axial stiffness of braces with the yielding core length; and (b) higher mode buckling order with the core plate thickness

yielding strengths to the Euler buckling strength in compression as follows

$$f_y R_y A_c = n^2 \pi^2 E I_c / L_c^2 \quad (9)$$

Where, f_y and R_y are the material yield strength and the over-strength factor of the core segment, and I_c is the moment of inertia of the core section. For single core BRB with rectangular cross-section of thickness, t_c, the value of n can be found as follows

$$n = \frac{L_c}{t_c} \sqrt{\frac{12 f_y R_y}{\pi^2 E}} \quad (10)$$

Wu *et al.* (2014) showed that a single higher mode compression wavelet may extend a length of 8-12 times the core plate thickness, t_c for loading corresponding to the axial strain of 2-4%. Fig. 2(b) shows the relationship between n and t_c for different values of L_c assuming f_y as 248 MPa, R_y as 1.3, and E as 200 GPa retrieved from Eq. (10). Thus, one can determine the minimum yielding length of BRBs by relating the value of n with the length of single wavelet corresponding to the design axial strain level. Out of the two approaches as discussed above, the maximum computed length of L_c should be considered as the limiting required length of yielding core segments. For example, let's consider a BRB of L_c equal to 5000 mm (~0.7L). The value of D_{by} can be computed as 8.06 mm as per the given data in the Fig. 2(b). Assuming the values of K_p and C_p are 0.21 and 0.485, respectively, the minimum value of L_c can be estimated as 1457 mm using Eq. (8). Alternatively, using Fig. 2(b), the value of n can be found as 7 for the value of t_c equal to 25 mm. Taking the single wave length as 12t_c (300 mm), the minimum yielding length of BRB is computed as 2100 mm considering the higher mode compression yielding. Hence, the limiting value of L_c can be taken as 2100 mm (~ 0.3L).

4. Analytical study

4.1 Details of study frames

Two buildings (i.e., 3-story and 6-story), as shown in Fig. 3, are considered for the analytical investigations in this study. These buildings are assumed to be located in Los Angeles, USA. The 3-story building is consisted of six bays along the longer direction and four bays along the shorter direction, whereas the 6-story building is consisted for five bays in both directions. The width of each bay is 9.14 m for both the buildings. It is assumed that all braced bays are located along the perimeters bays of the buildings. There are four and six braced bays along any direction of the 3- and 6-story buildings, respectively. Typical height of each story of both buildings is 3.96 m except the first story of the 6-story building which is 5.49 m in height. The buildings

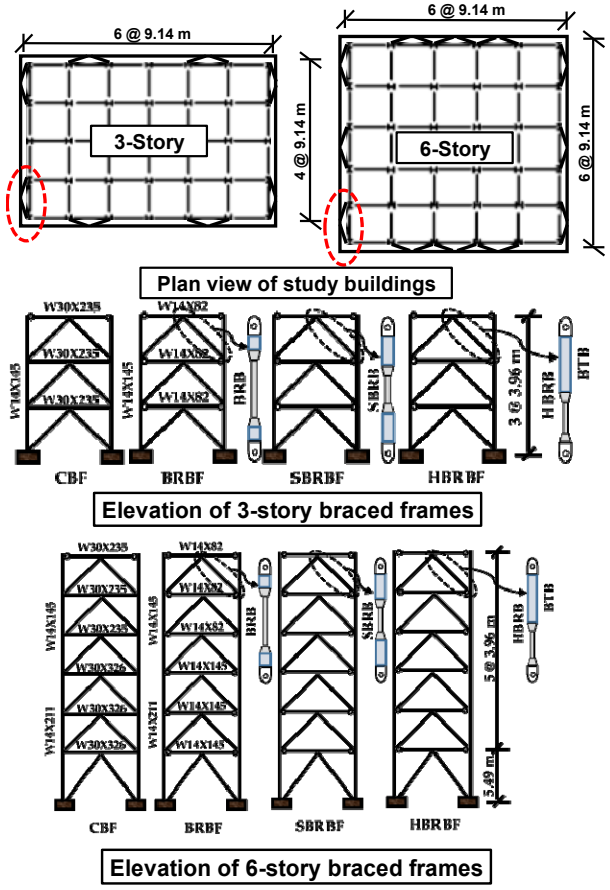

Fig. 3 Plan layout of 3- and 6-story study buildings and elevation of braced frames

Table 1 Details of sections and effective elastic stiffness of braces used in the braced frames

Story	3VCBF	3VBRBF	3VSBRBF	3VHBRBF	
3-story	BTB	$K_{e\,(BRB)}$ (kN/cm)	$K_{e\,(SBRB)}$ (kN/cm)	$K_{e\,(HBRB)}$ (kN/cm)	BTB
3rd	HSS5X5X3/8	1095	1491	1724	HSS12X12X1/2
2nd	HSS6X6X1/2	1642	2237	2586	HSS12X12X1/2
1st	HSS6X6X1/2	1970	2684	3103	HSS12X12X1/2
Story	6VCBF	6VBRBF	6VSBRBF	6VHBRBF	
6-story	BTB	$K_{e\,(BRB)}$ (kN/cm)	$K_{e\,(SBRB)}$ (kN/cm)	$K_{e\,(HBRB)}$ (kN/cm)	BTB
6th	HSS5X5X5/16	665	907	1048	HSS12X12X1/2
5th	HSS6X6X1/2	967	1316	1522	HSS12X12X1/2
4th	HSS6X6X1/2	1306	1779	2057	HSS12X12X1/2
3rd	HSS7X7X1/2	1554	2118	2449	HSS16X16X1/2
2nd	HSS7X7X1/2	1718	2341	2751	HSS16X16X1/2
1st	HSS8X8X1/2	1514	2063	2384	HSS16X16X1/2

are designed based on the FEMA 450 (2003) and ASCE 7-10, 2010) guidelines along with the applicable seismic provisions as per ANSI/AISC 341-10 (2010) and ANSI/AISC 360-10 (2010). Site class "D" with the design spectral acceleration (S_{DS} and S_{D1}) values corresponding to the short (0.2s) and long (1.0s) periods are assumed as 1.393 g and 0.77g, respectively. For both 3- and 6-story buildings, four types of braced frames are considered in this analytical study, namely, (i) frames with conventional BRBs (BRBFs); (ii) frames with SBRBs (SBRBFs); (iii) frame with HBRBs (HBRBFs); and (iv) frames with conventional BTBs (CBFs). It is assumed that all braces are arranged in the inverted-V configurations. The braced frames are represented as 3VBRBF, 6BRBF, etc. The values of response reduction factor (R) are assumed as 6 and 8 for CBFs and all other frames, respectively.

The approximate time period (T_a) of building frames is calculated as per ASCE 7-10 (2010) specification as follows

$$T_a = C_t h_n^{\,x} \tag{11}$$

Where, C_t = 0.0488 (CBFs) and 0.0731 (BRBFs); x = 0.75; h_n = height of the building; For 3-story frames, the value of T_a is computed as 0.31s for CBF and 0.47s for other frames. The corresponding values for the 6-story frames are 0.55s and 0.83s. The design base shear (V) of the buildings is computed as follows

$$V = C_s W \tag{12}$$

Where, W is the seismic weight of the buildings, and C_s is the seismic response coefficient. The value of W is computed as 26983 kN and 56065 kN for the 3- and 6-story buildings, respectively. For the 3-story frame, the values of C_s are computed as 0.24 (3VCBF) and 0.18 (other frames). The corresponding values for the 6-story frames are 0.23 and 0.12. The distribution of seismic forces over the height of the buildings is carried out as per ASCE-7 (2010) guidelines. In addition, an accidental eccentricity of 5% has been considered in the design of braced frames.

4.2 Design of frame members

Braces at any story level are designed for the forces obtained by resolving the story shear corresponding to the design base shear. The end connections for the braces of CBFs are considered as pinned with the effective length factor as 0.85 assuming their out-of-plane buckling. Hollow structural steel (HSS) sections are used as braces such that their width-to-thickness (d/t) ratio value satisfy the local buckling criteria for the highly ductile members as per ANSI/AISC 341-10 (2010) provisions. The material yield stress (f_y) and over-strength factor (R_y) for BTBs are assumed as 317 MPa and 1.1, respectively. Post-buckling strength of BTBs is assumed as 30% of their buckling strength. The corresponding values of f_y and R_y for the BRBs are considered as 248 MPa and 1.3. The values of adjustment factors in tension (ω) and compression (β) for BRBs are taken as 1.4 and 1.1, respectively (Sahoo and Chao 2010). The maximum design forces in tension and compression of BRBs are computed as $\omega R_y f_y A_c$ and $\beta\omega R_y f_y A_c$, respectively. Both experimental and finite element investigations concluded that the values of ω and β are independent of the yielding core lengths of BRBs (Pandikkadvath and Sahoo 2016a, b). Hence, the same values of ω and β are considered for BRBs, SBRBs, and HBRBs. The BTB segment of HBRB is designed for a yielding/buckling force higher than the expected ultimate tensile/compressive force in the BRB segment in order to limit the inelastic deformations limited to BRB segments only. Pending further study, the ratio of elastic axial strengths of BTBs to the expected peak strengths of BRBs has been assumed as 2 in this study. Further, the connections between the BRB and BTB segments of HBRBs are assumed perfectly rigid without any shear lag effects. Beams and columns of the braced frames are dimensioned based on the capacity-based design approach. Beams are designed for axial force and bending moment due to the unbalanced axial strengths of braces in tension and compression and the gravity loadings corresponding to the critical load combinations. Columns are designed for the axial load and bending moment obtained using column-tree

approach for the maximum expected strengths of braces and beams. The values of f_y and R_y for the beams and columns are assumed as 345 MPa and 1.1, respectively. Table 1 summarizes the brace sections and their properties used in the braced frames. Fig. 3 shows the structural sections used as beams and columns of the braced frames considered in this study.

4.3 Modelling techniques

The nonlinear static and dynamic response of the planar braced frames considered in this study is evaluated using a computer software PERFORM-3D (CSI 2013). Beams and columns are modelled as frame elements with the nonlinear properties represented by bi-linear lumped plasticity models (FEMA 356 2000). Both the moment-rotation (M-θ) and the axial load-moment interaction (P-M-M) plastic hinges are assigned to these members at the critical locations. Panel zones at the beam-column joints are modeled as a series of nonlinear springs along with the rigid end offsets at the beam/column ends. BTBs are modelled as inelastic beam fiber elements using the buckling-type materials. BRB elements inbuilt in the PERFORM-3D (CSI 2013) are used to model the BRB components of the braced frames. In case of the conventional BRBs, the values of L_c, L_t, and L_j are taken as 70%, 6% and 24% of their work-point lengths. The values of A_t and A_j are assumed as 2.5 and 3.5 times the value of A_c for the conventional BRBs. For both SBRBs and HBRBs, the value of L_c is taken as 40% of their work-point lengths using Eq. (11) and Fig. 2(b). The cross-sectional area of elastic transition zones of SBRBs/HBRBs are kept same as that of the BRBs. The values of L_j for SBRBs and HBRBs are considered as 54% and 24% of their working point lengths, respectively. The values of effective stiffness of braces of various braced frames are summarized in Table 1. A post-yield stiffness of $0.25K_e$ has been assumed for BRBs, whereas, for SBRBs and HBRBs, a post-yield stiffness of $0.3K_e$ is adopted based on the results of past studies by Pandikkadavath and Sahoo (2016a, b). Both kinematic and isotropic (combined) hardening behavior are considered in the material modelling of BRBs. Fig. 4(a) shows the comparison of the predicted hysteretic response of BTBs with the results of Black *et al*. (1980) and BRBs with a past study by Merritt *et al*. (2003).

A leaning column is modeled to account for the P-Delta effect due to the gravity loading on the seismic response of the braced frames. This column is connected to the braced frame models using rigid links at each floor level. A Rayleigh damping of 2% is considered in the analysis of all braced frames. A suite of twenty ground motions representing the DBE (LA 1-20) and MCE (LA 21-40) hazard levels has been selected for the nonlinear dynamic analyses (Somerville *et al*. 1997). These ground motions are amplitude-scaled to match the response spectra with the design spectrum corresponding DBE and MCE hazard levels as shown in Fig. 4(b). The MCE level design spectra is obtained by amplifying the DBE level spectra by 50%.

5. Analysis results

As stated earlier, both non-linear static and dynamic analyses are conducted to determine the lateral strengths, yield mechanisms, drift response, and brace ductility demand of the braced frames. The first mode time period obtained from the analysis are 0.44s, 0.55s, 0.53s and 0.49s for 3VCBF, 3VBRBF, 3VSBRBF and 3VHBRBF respectively and 0.73s, 1.01s, 0.98s and 0.95s respectively

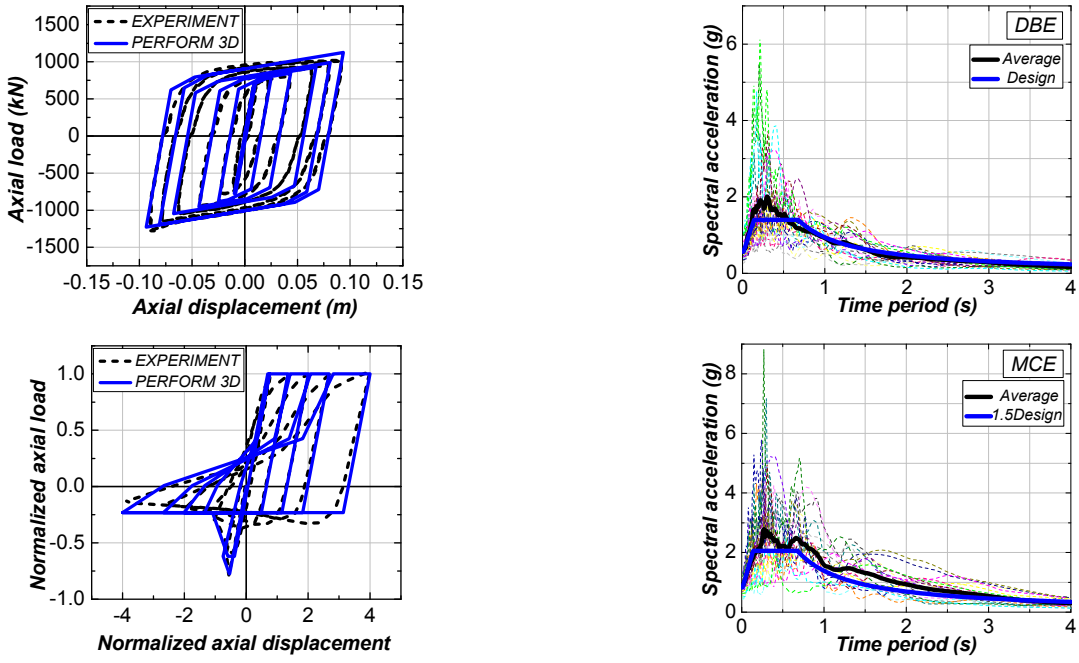

(a) (b)

Fig. 4 Comparison of (a) predicted hysteretic response of BRB and BTB with test results; and (b) response spectra of DBE and MCE ground motions with design spectra

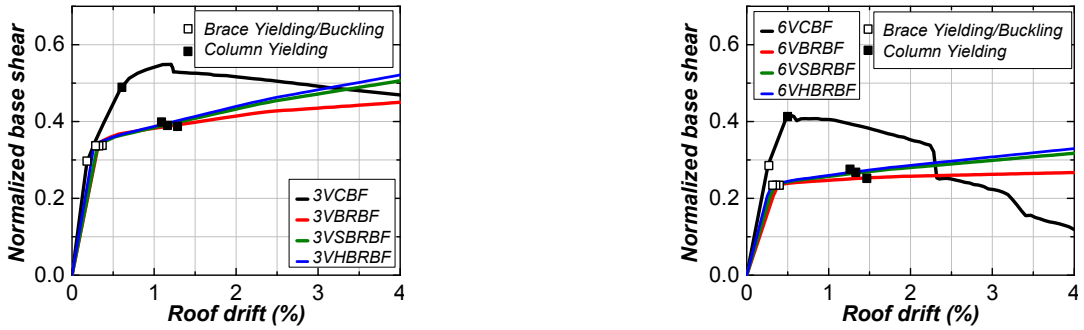

(a) (b)

Fig. 5 Comparison of base shear vs. roof drift response of (a) 3-story and (b) 6-story frames

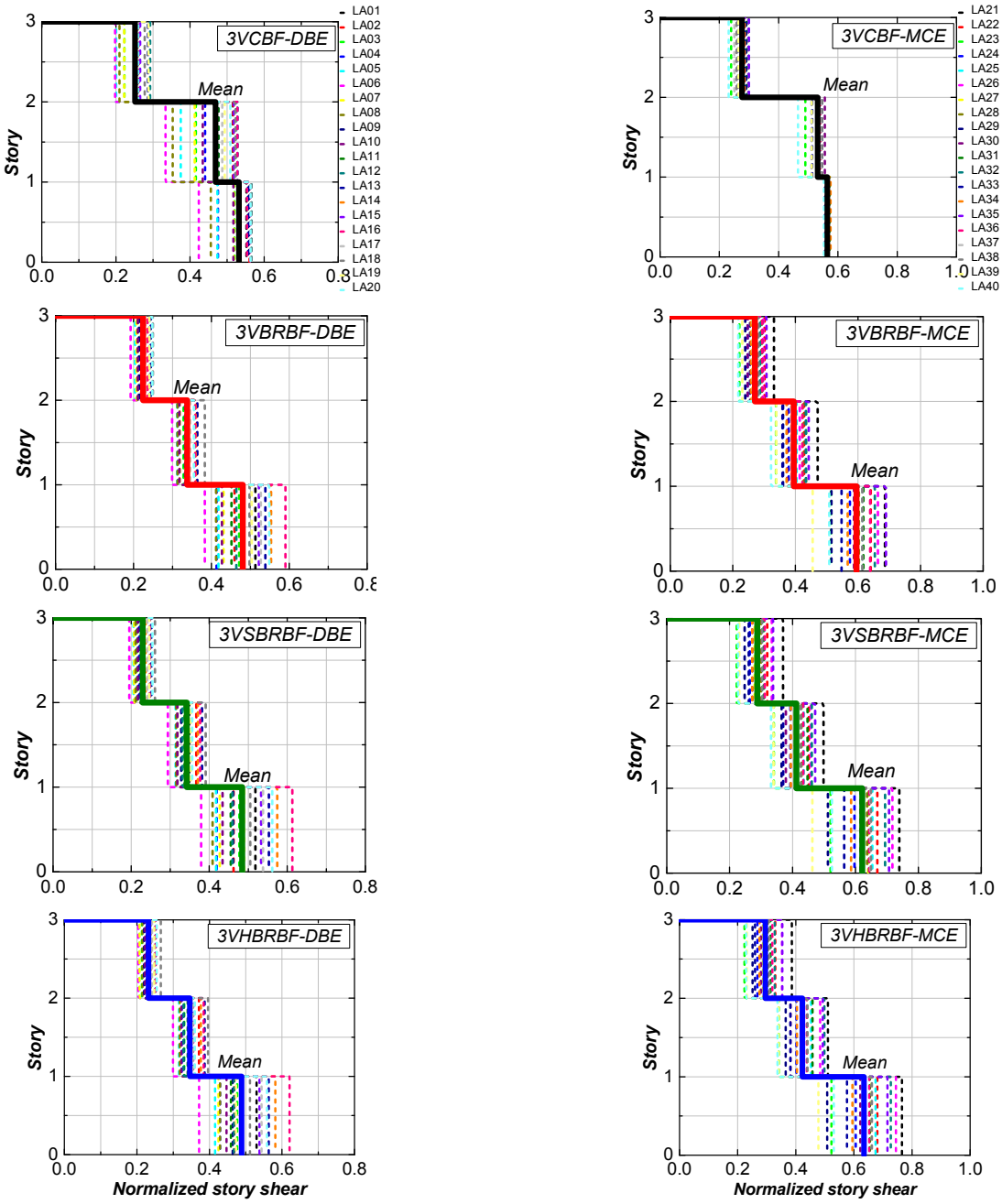

(a) (b)

Fig. 6 Variation of normalized base shear along the story height of 3-story braced frames under (a) DBE; and (b) MCE level ground motions

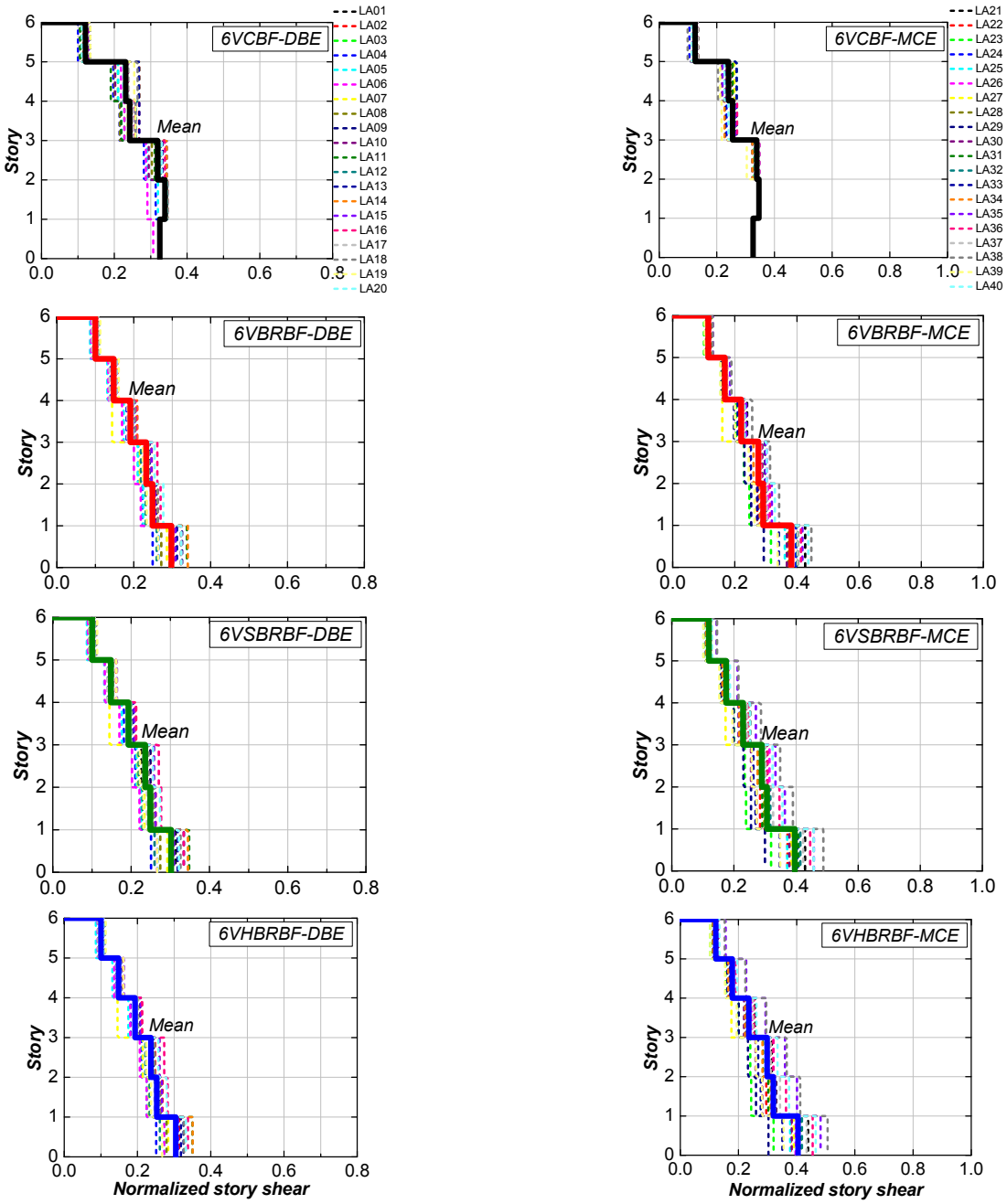

(a) (b)

Fig. 7 Variation of normalized base shear along the story height of 6-story braced frames under the (a) DBE and (b) MCE level ground motions

for 6VCBF, 6VBRBF, 6VSBRBF and 6VHBRBF. This shows the proposed modification increases the system stiffness and it may improve the non-linear response associated with the brace system. The analyses results are discussed in the following sections.

5.1 Lateral strength vs. roof drift response

Fig. 5 shows the variation of base shear with the roof drift of the braced frames. The base shear values are normalizes with respect to their seismic weights. As expected, the CBFs exhibited the higher initial lateral stiffness as compared to other braced frames. For both 3-story and 6-story frames, the initial lateral stiffness of CBFs is found to be 1.7 times that of the BRBFs. The initial lateral stiffness values for the SBRBFs and HBRBFs are nearly 1.1 and 1.3 times the values for the respective BRBFs. The buckling of braces in 3VCBF and 6VCBF is noted at the roof drift of 0.2% and 0.25%, respectively. The yielding of BRBs is noticed at nearly same value of roof drifts of BRBFs, SBRBFs and HBRBFs. The yielding of column bases of 3VCBF and 6VCBF is noticed at the roof drift of 0.6% and 0.5%, respectively. However, the column yielding in the braced frames with BRBs is delayed as compared to the CBFs. For the 3-story frames with BRBs, the column yielding is observed nearly at the roof drift of

1.25%. Among three BRBFs considered in this study, 3VHBF exhibited the column yielding earlier than the 3VSBRBF and 3VBRBF. The same trend in the column yielding is also noticed in the 6-story frames with BRBs at the roof drift of 1.5%. In the post-elastic stage, both 3VCBF and 6VCBF exhibited strength and stiffness degradation beyond the roof drift of 1% due to the buckling of compression braces and the formation of plastic hinges in the columns at the ground story level leading to their soft-story collapse. For all braced frames with BRBs, strain-hardening effect is noticed in their post-yielding stages up to the roof drift of 4%.

5.2 Story shear response

Nonlinear dynamic analyses are conducted to study the variation of story shear demand over the height of 3- and 6-story braced frames under the forty selected ground motions. In case of BRBFs, the story shear resistance is provided only by the BRBs due to very limited damages to

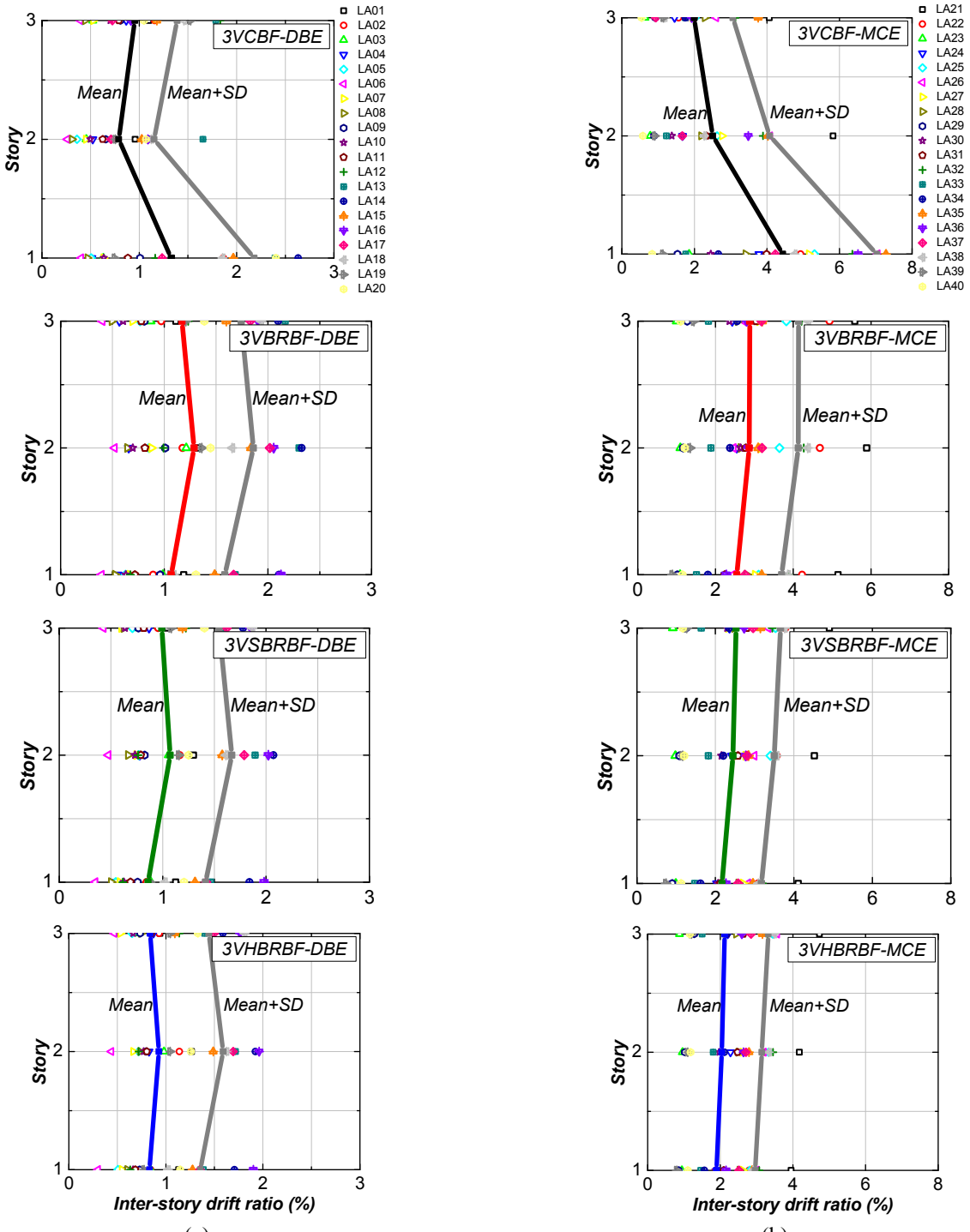

(a) (b)

Fig. 8 Inter-story drift response along the story height for 3-story braced frames under DBE and MCE hazard levels

the beams and columns under DBE level ground motions (Sahoo and Chao 2015). This study also confirmed that there is a gradual increase in the story shear demand from top to bottom stories under both DBE and MCE level ground motions for all the braced frames except the 3VCBF and 6VCBF. Figs. 6 and 7 shows the average (Mean) variation of peak values of story shear demand at various story level of 3- and 6-story braced frames under the DBE and MCE level ground motions. In case of 3VCBF, the average values of story shear demand at the first and second story levels are comparable and are significantly higher than the top story. This effect is more prominent in case of MCE level ground motions as shown in Fig. 6(b) indicating that the conventional steel braces at the third story are underutilized. In case of 6VCBF, the average story shear in bottom three stories are significantly higher that top three stories as shown in Figs. 7(a) and (b) under the DBE as well as MCE level ground motions. The maximum value of story shear is noticed at the second floor level as compared to the first story. The absolute maximum values of normalized story shear demand under the DBE level ground motions are found to be 0.57, 0.59, 0.61 and 0.62 for 3VCBF, 3VBRBF, 3VSBRBF and 3VHBRBF, respectively. Similarly, the corresponding values for the 6-story frames are noted as 0.34, 0.34, 0.35, and 0.36. Similar variation in the maximum value of story shear demand is noted for 3- and 6-story braced frames under the MCE level ground motions. This shows that there is no significant change in the story shear demand between the CBFs and BRBFs with conventional BRBs or short core BRBs.

5.3 Interstory drift response

Inter-story drift ratio (ISDR) is defined as the ratio of relative lateral displacement of a story to its corresponding story height. ISDR response is an indirect measurement of structural damage due to an earthquake. The maximum value of ISDR for 3VCBF under DBE level is noted as 3.3% at the first story level for the LA16 ground motion, whereas the maximum values of ISDR are 3VBRBF and 3VSBRBF are found to be 2.3% and 2.1% at the second story level under the LA14 ground motion, respectively. Similarly, the corresponding value for 3VHBRBF is noted as 1.9% under the LA16 ground motion. Fig. 8(a) shows the statistical (i.e., Mean and Mean + standard deviation (SD)) values of ISDR for 3-story braced frames under DBE level ground motions. The average values of maximum ISDR for 3VCBF, 3VBRBF, 3VSBRBF and 3VHBRBF are 1.3%, 1.3%, 1.1% and 0.9%, respectively. Except 3VCBF, all other braced frames showed the maximum ISDR response at the second story level. The maximum reduction in the ISDR response is noted as 17% and 28% for the 3VSBRBF and 3HBRBF as compared to the 3VBRBF, respectively. Similar variation in the ISDR response is noticed for the 3-story braced frames under the MCE level ground motions as shown in Fig. 8(b).

3VCBF exhibited the maximum and average ISDR values of 9.3% and 4.4%, respectively. The average values of ISDR for 3VBRBF, 3VSBRBF, and 3VHBRBF are found to be 2.9%, 2.5% and 2.1%, respectively. Fig. 9 shows the ISDR response of the 6-story braced frames under the DBE and MCE level ground motions. The maximum value of ISDR for the 6VCBF is noted as 3.8% at the first story level under the LA16 ground motion. The corresponding values for the 6VBRBF, 6VSBRBF and 6VHBRBF are noted as 2.4%, 2.2% and 1.9% at the first story level, respectively (all were under LA15). The average values of ISDR under the DBE level ground motions are observed as 1.6%, 1.3%, 1.2% and 1.0% for the 6VCBF, 6VBRBF, 6VSBRBF and 6VHBRBF, respectively. The corresponding values are noted as 4.3%, 2.9%, 2.6% and 2.4% under the MCE level ground motions. The mean values of ISDR response of all the braced frames except 3VCBF are smaller than the limiting value of 1.5% under DBE hazard levels as per ASCE/SEI 41-06 (2006) guidelines. This shows a significant reduction in the ISDR response for the 3- and 6-story braced frames with BRBs as compared to the CBFs under the MCE level ground motions. Further, the use of short-core BRBs resulted in the reduction of mean ISDR response in the range of 20-30%.

5.4 Residual drift response

The main focus of this study is to quantify the reduction in residual drift ratio (RDR) response of the braced frames under the earthquake loading. RDR is the ratio of the relative residual lateral displacement of a story to its height. The excessive RDR response of a structure makes it difficult for retrofitting and reusability in the post-earthquake scenario. Fig. 10 shows the variation of statistical values of RDR response of the 3-story braced frames under the DBE and MCE level ground motions. 3VCBF exhibited an absolute maximum RDR value of 1.4% under the LA13 ground motion and a peak average RDR value of 0.3% at the first story level under the DBE level ground motions. 3VBRBF exhibited an absolute maximum and peak average RDR value of 1.4% and 0.5% under the DBE level ground motions. The peak values of average RDR for the 3VSBRBF and 3VHBRBF are noted as 0.4% and 0.3%, respectively. While the residual drift response of the 3VCBF is noted at the bottom stories, all BRBFs exhibited the higher value of RDR at the top story levels. As shown in Fig. 10(b), under MCE level, the peak values of average RDR for 3VCBF, 3VBRBF, 3VSBRB and 3VHBRBF are noted as 2.2%, 1.6%, 0.9% and 0.8%, respectively, indicating a reduction of 50% for HRBF as compared to the corresponding BRBF.

Fig. 11 shows the statistical values of RDR response at different story levels of the 6-story braced frames under the DBE and MCE level ground motions. For 6VCBF under DBE level ground motions, the absolute maximum and peak average RDR values are noted as 1.2% and 0.4% at the first story level. For the braced frames with BRBs, the maximum residual drift is noted the top story level. The peak value of average RDR is reduced from 0.6% for 6VBRBF to 0.42% and 0.36% for the 6VSBRBF and 6VHBRBF, respectively. The use of short core BRBs reduced the peak residual drift response in the range of 25-35%. The peak values of average RDR response are 1.5%, 1.7%, 1.2% and 1.0% for 6VCBF, 6VBRBF, 6VSBRBF and 6VHBRBF, respectively, under the MCE level ground motions. In this case, the maximum reduction in RDR is

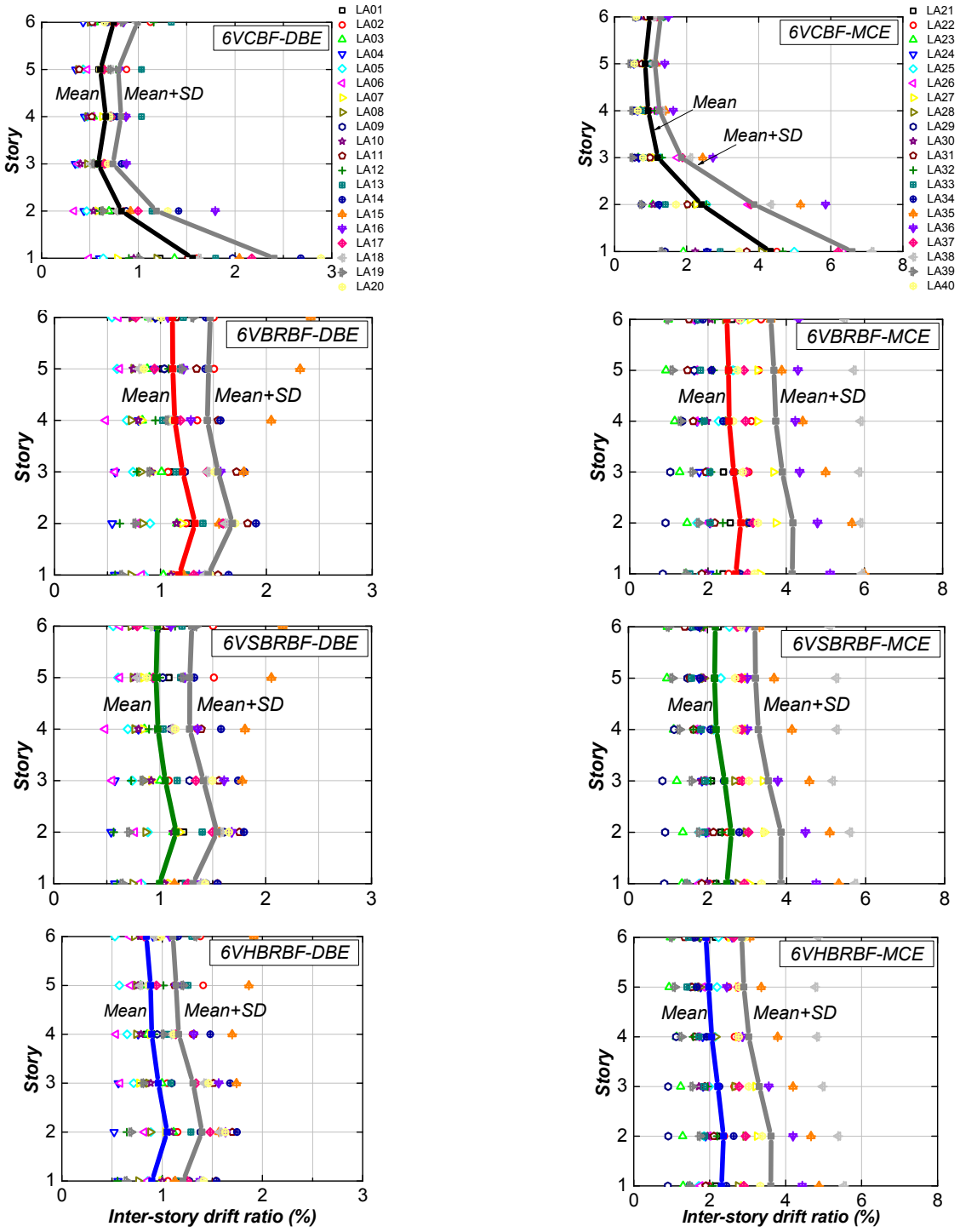

(a) (b)

Fig. 9 Inter-story drift response along the story height for 6-story braced frames under DBE and MCE hazard levels

noted in the range of 30-40% for the frames with short-core BRBs as compared to the BRBF. The allowable values of RDR under the DBE and MCE level earthquakes are 0.5% and 2%, respectively (ASCE/SEI 41-06 2006). The peak values of RDR are within the limiting values for the braced frames except 3VCBF.

5.5 Displacement ductility and cumulative ductility demand

One of the main concerns associated with the BRBs of short yielding core lengths is their ability to meet the ductility requirements under seismic loading since the ultimate deformation of BRBs core is reduced with the reduction in their lengths. Though the low-cycle capacity and the higher mode compression buckling requirements have been adopted in this study for determining the length of short core BRBs, their validity need to be checked with the experimental results. Past studies showed that the

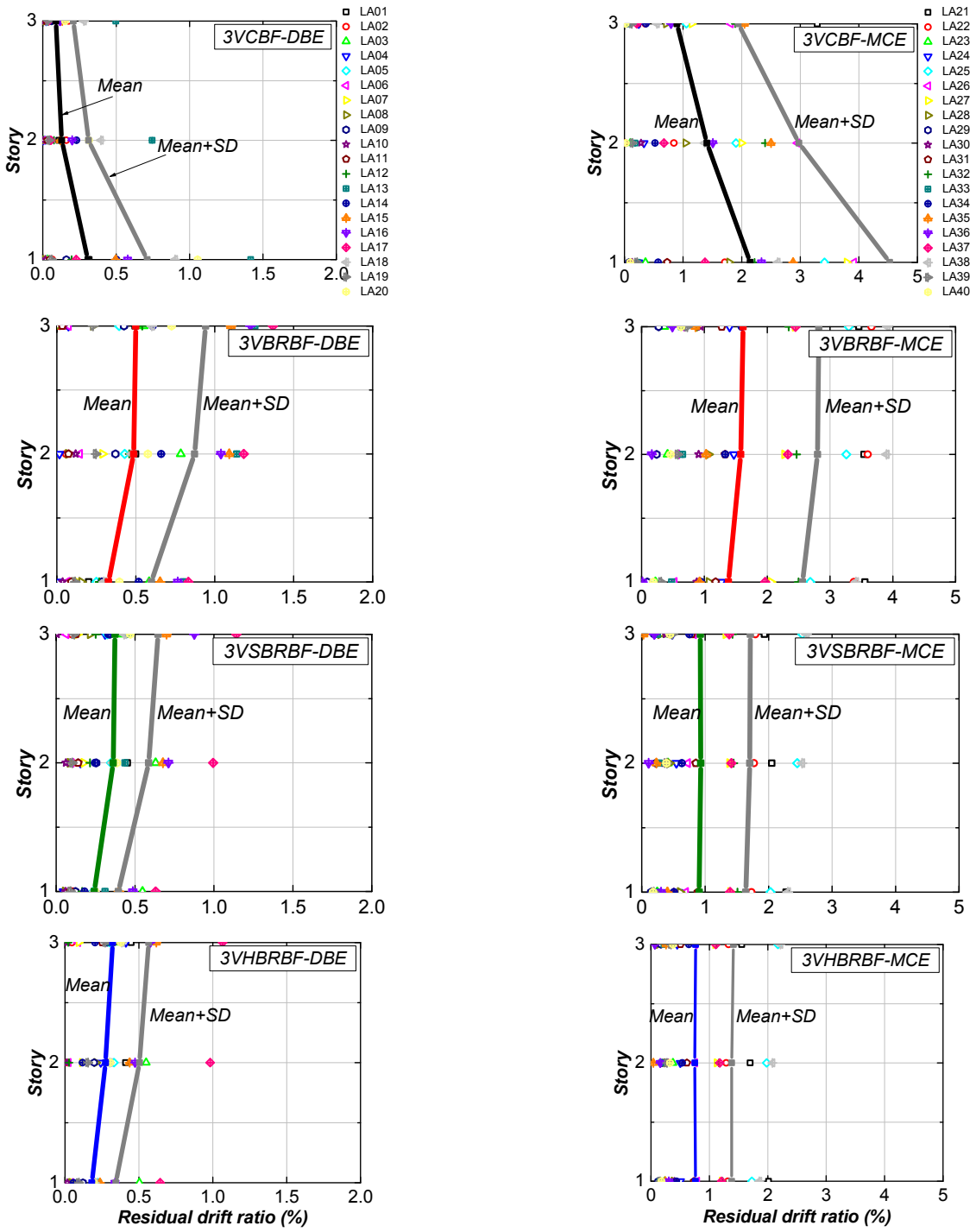

(a) (b)

Fig. 10 Residual drift response along the story height for 3-story braced frames under DBE and MCE hazard levels

conventional BRBs are capable of achieving the maximum displacement ductility (μ_{mxm}) of 25 and the cumulative displacement ductility (μ_{cum}) of more than 400 without any instability (Usami *et al*. 2003). Merritt *et al*. (2003) showed that the corresponding values for the BRBs are 15 and 1600.

In this study, the limiting values of μ_{mxm} are 15 and 25 under the DBE and MCE level ground motions, respectively. Similarly, the corresponding limiting values of μ_{cum} are considered as 200 and 400. Fig. 12 shows the variation of maximum ductility demand on the 3- and 6-story braced frames under the DBE and MCE level ground motions. The absolute maximum values of μ_{mxm} for 3VBRBF, 3VBRBF, 3VSBRBF and 3VHBRBF are found to be 11.2, 17.1 and 15.8, respectively, under the DBE level ground motions. The corresponding average value of μ_{mxm} are computed as 6.7, 9.5 and 8.9. The maximum displacement ductility demand is increased in case of the braced frames with short core BRBs as compared to the conventional BRBs, though the average values of μ_{mxm} for

all the BRBFs are less than the limiting value of 15. Similar ductility demand on BRBs is noted for the 6-story braced frames under the DBE level ground motions. The average values of μ_{mxm} for 6VBRBF, 6VSBRBF and 6VHBRBF are noted as 7.3, 10.7 and 9.5, respectively. The maximum values of μ_{mxm} for 3VBRBF, 3VSBRBF and 3VHBRBF under the MCE level ground motions are found to be 27.2, 36.9 and 34.2, respectively. The corresponding average values of μ_{mxm} are computed as 13.9, 20.7 and 18.8. The absolute values of μ_{mxm} for the 6-story braced frames are noted as 28.5, 46.2, and 42.4, whereas the average values of μ_{mxm} are computed as 14.8, 22.3 and 20.1 for 6VBRBF, 6VSBRBF and 6VHBRBF, respectively. This shows that the average values of μ_{mxm} for the 6-story frames are less than the limiting value of 25.

Fig. 13 shows the variation of cumulative displacement ductility (μ_{cum}) demands on BRBs of 3- and 6-story braced frames under the DBE and MCE level ground motions. The maximum values of μ_{cum} for 3VBRBF, 3VSBRBF and 3VHBRBF are found to be 86, 152 and 139, under the DBE

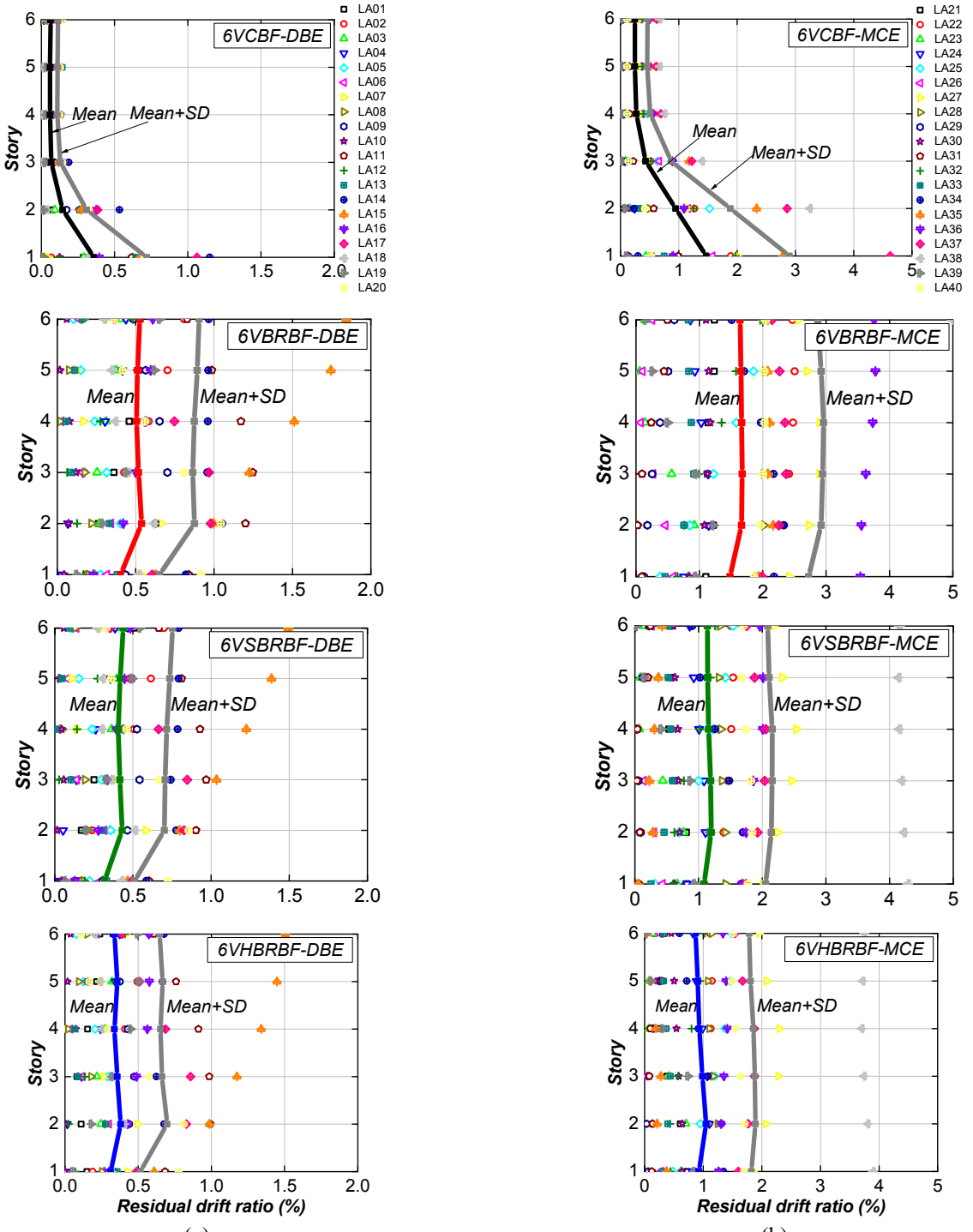

(a) (b)

Fig. 11 Residual drift response along the story height for six-story braced frames under DBE and MCE hazard levels

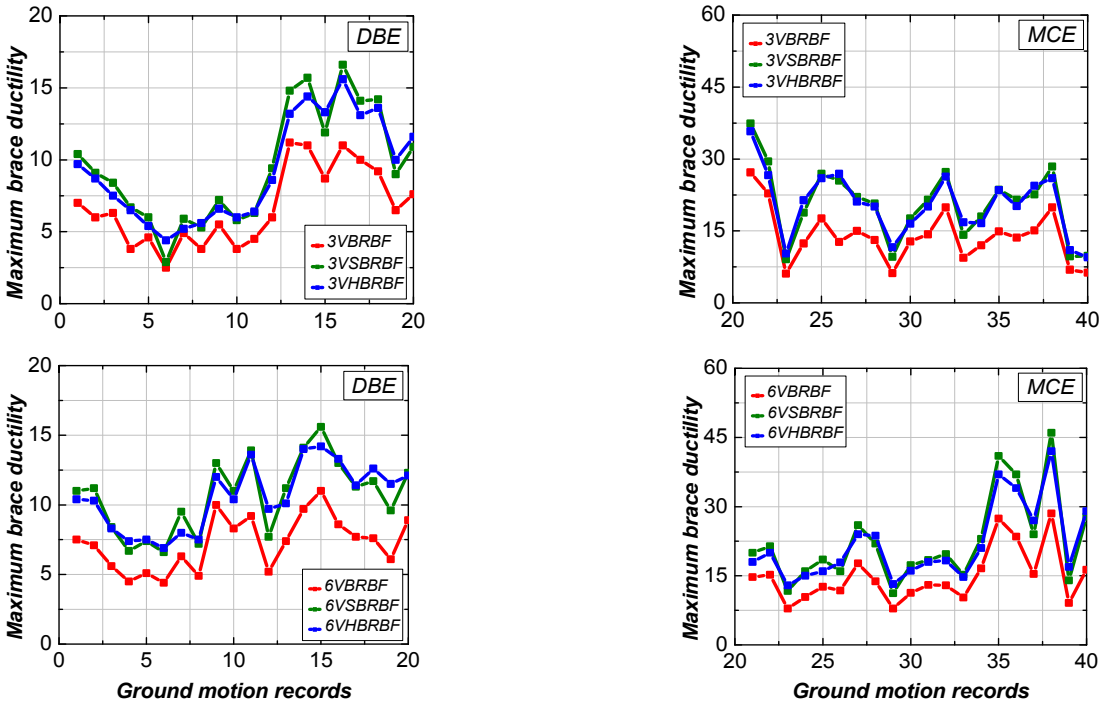

Fig. 12 Maximum displacement ductility demand on BRBs of 3- and 6-story braced frames under (a) DBE; and (b) MCE level ground motions

level ground motions, respectively. The corresponding average values of μ_{cum} are computed as 43, 69 and 63. Similarly, the maximum values of μ_{cum} for 6VBRBF, 6VSBRBF and 6VHBRBF under the DBE level ground motions are noted as 82, 134 and 121, respectively. The corresponding average values of μ_{cum} are calculated as 41, 67 and 59. Under the DBE hazard level, the average values of μ_{cum} in all cases are less than the limiting value of 200.

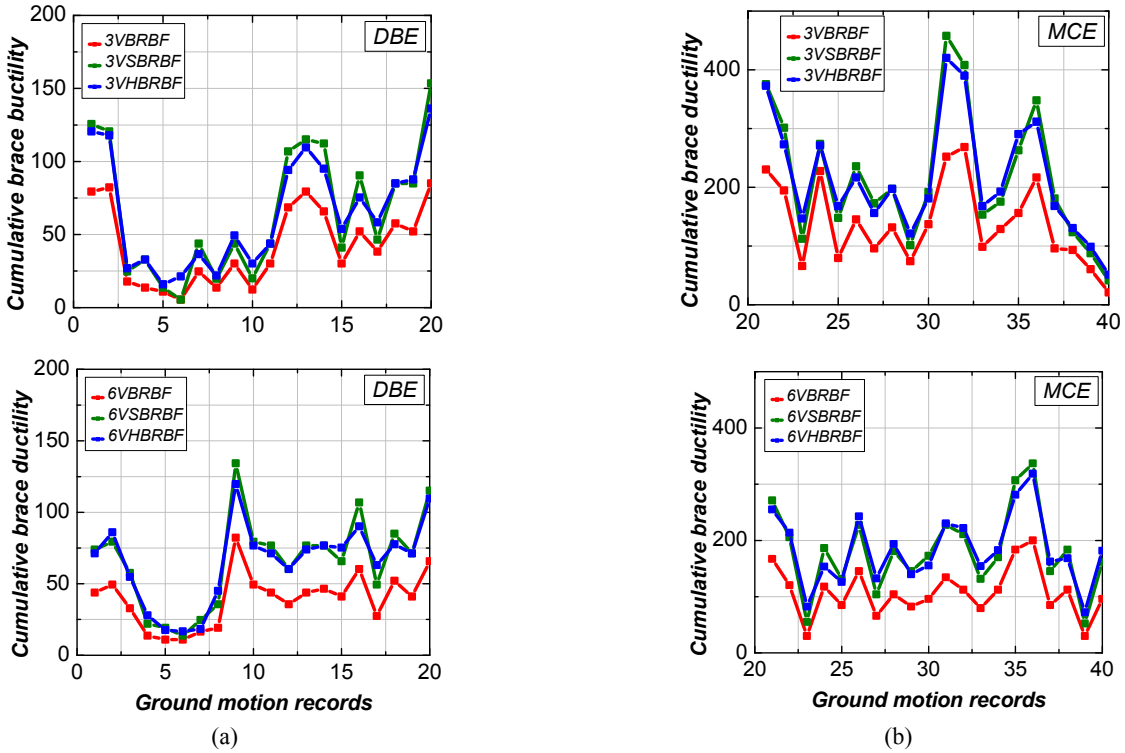

Fig. 13 Maximum cumulative ductility demands on BRBs of 3- and 6-story braced frames under (a) DBE; and (b) MCE level ground motions

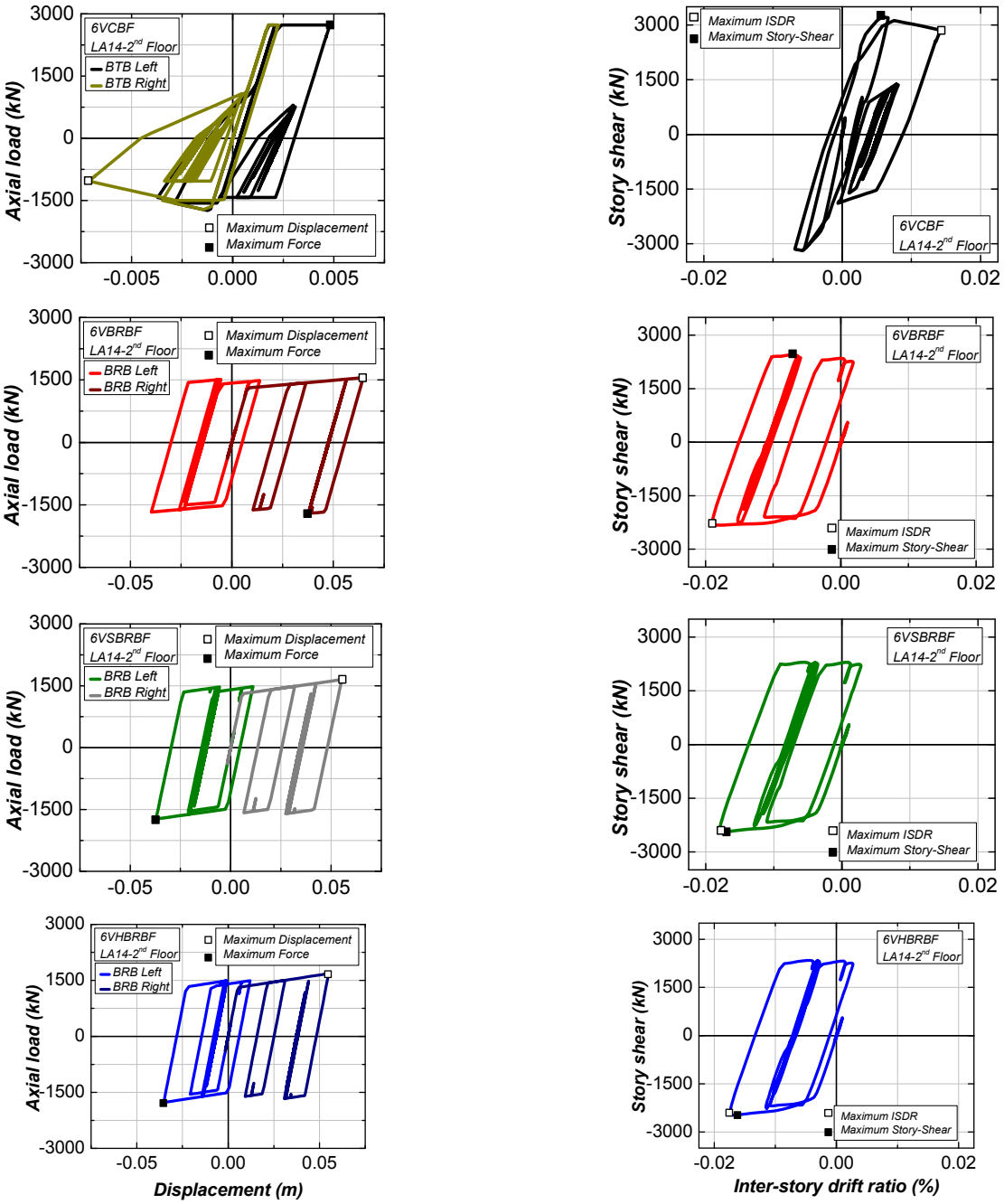

Fig. 14 (a) Brace hysteresis and (b) story shear variation with the ISDR response at second story level of 6-story braced frames under LA14 ground motion

The maximum values of μ_{cum} of 3VBRBF, 3VSBRBF and 3VHBRBF under the MCE level ground motions are 269, 457 and 421, respectively. The corresponding average values of μ_{cum} are computed as 138, 217 and 201. For the 6-story frames under the MCE level ground motions, the maximum values of μ_{cum} for 6VBRBF, 6VSBRBF and 6VHBRBF are noted as 201, 337 and 318, respectively. The corresponding average values of μ_{cum} are computed as 108, 191 and 178. Considering the limiting value of μ_{cum} to be 400 under the MCE level ground motions, both 3- and 6-story braced frames with BRBs exhibited sufficient cumulative displacement ductility capacity.

5.6 Seismic response under critical earthquake

In order to investigate the behaviour of BRBs in the braced frames under earthquake loading, the time-history response of 6-story braced frames under LA14 ground motion has been studied in detail. Fig. 14 shows the brace hysteresis and story shear vs. drift response of 6-story braced frames under LA14 ground motion. All BRBs exhibited the maximum ISDR response at the second story level under the selected ground motions. 6VBRBF exhibited a maximum ISDR of 1.9% with the maximum brace forces of 1553 kN (tension) and 1705 kN (compre-

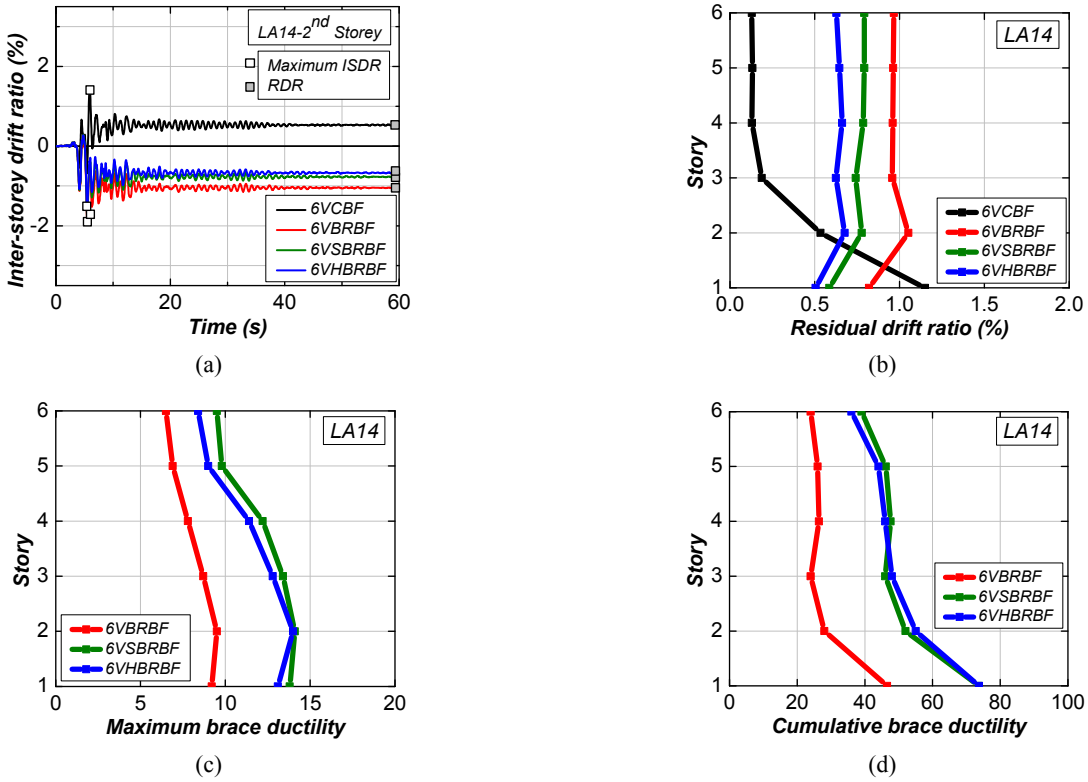

Fig. 15 (a) Drift vs. time response for second floor, (b) RDR response, (c) maximum displacement ductility, (d) cumulative displacement ductility demands of 6-story frames under LA14 ground shaking

ssion). Story stiffness is defined as the story shear to the corresponding lateral displacement in the elastic range. The values of elastic story stiffness at the second story level of 6VCBF, 6VBRBF, 6VSBRBF and 6VHBRBF are computed as 234 kN/mm, 82.3 kN/mm, 85.2 kN/mm, and 88.8 kN/mm, respectively. This indicated that 6VCBF is nearly 2.9 times stiffer as compared to BRBF. Though there is no significant increase (~8%) in the elastic stiffness due to the use of hybrid braces, RDR response of the braced frames with short-core BRBs is drastically reduced (~30-40%) at the second story level as compared to the conventional BRBF, as shown in Fig. 15. Because of low post-yield stiffness of BRBs, BRBFs continue to vibrate about a deflected position resulting in a shift in the hysteretic response away from the initial zero position. Hence, the hysteretic response for BRBFs are one sided a shown in Fig. 14. However, this is not the case for the CBFs due to the re-centering capability of conventional braces in the post-buckling stages.

All BRBs showed the maximum ductility demand at the second story and the cumulative maximum ductility demand at the first story levels of the 6-story frame. The maximum displacement ductility demand on BRBs of 6VBRBF, 6VSBRBF and 6VHBRBF are 9.7, 13.9 and 14.1, respectively. The corresponding values of cumulative displacement ductility demands are 46.6, 76.7, and 79.8. All the 6-story frames exhibited the smaller cumulative displacement ductility demands at the top story levels. This shows that the use of short-core BRBs reduced the drift response of the braced frames while marginally increasing the ductility demand on BRBs.

6. Conclusions

This study is focussed on determining the limiting core lengths of BRBs required for effective seismic performance of the braced frames using the fatigue as well as the higher mode compression buckling criteria. The main of this study is to evaluate the effectiveness of short-core BRBs in controlling the post-earthquake residual drift response of the braced frames. Nonlinear static and dynamic analyses have been carried out for the 3- and 6-story braced frames with conventional steel braces, BRBs, short-core BRBs and hybrid BRBs arranged in the inverted-V (chevron) configurations. A suite of forty ground motions representing the DBE and MCE hazard levels are used for nonlinear dynamic analyses of all the braced frames.

The following conclusions can be drawn from this study:

- The minimum length of yielding core required for a BRB should be computed based on the fatigue requirement using Coffin-Manson relationship and the higher mode compression buckling criteria. The minimum length of BRB core is found to be 30% of the length between work points for a conventional BRBs in chevron configuration.
- The linear elastic stiffness of the braced frames is increased in the range of 15-30% by reducing the length of yielding core segments of conventional BRBs or using the short-core BRBs in series with conventional steel brace. However, there is no significant change noted in the story shear variation

over the height of the braced frames under the dynamic loading conditions.

- The use of short-core BRBs reduced the inter-story drift ratio (ISDR) response in the range of 15-25% for the 3- and 6-story braced frames under DBE and MCE level ground motions. However, the reduction in the residual drift ratio (RDR) response is noted in the range of 25-45% for the BRBFs with short-core BRBs. The maximum reduction in the RDR response is noted for the hybrid BRBFs fitted with short-core BRBs in series with the conventional steel braces.
- The maximum displacement ductility demand on BRBs is increased as the yielding core lengths are reduced. The increase in the displacement ductility demand is found to be in the range of 1.5 and 1.3 times for the SBRBFs and HBRBFs, respectively, as compared to the conventional BRBFs. However, there is significant increase in the cumulative displacement ductility demand due to the reduction in the yielding core lengths of BRBs.

References

Aiken, I.D., Mahin, S.A. and Uriz, P.R. (2002), "Large-scale testing of buckling-restrained braced frames", *Proceedings of Japan Passive Control Symposium*, Tokyo Institute of Technology, Japan.

ANSI/AISC 341-10 (2010), Seismic provisions for structural steel buildings; American Institute of Steel Construction, Chicago, IL, USA.

ANSI/AISC 360-10 (2010), Specifications for structural steel buildings; American Institute of Steel Construction, Chicago, IL, USA.

ASCE/SEI 41-06 (2006), Seismic rehabilitation of existing buildings; American Society of Civil Engineers, Reston, VA, USA.

ASCE/SEI 7-10 (2010), Minimum design loads for buildings and other structures; American Society of Civil Engineers, Reston, VA, USA.

Black, R.G., Wenger, W.A. and Popov, E.P. (1980), "Inelastic buckling of steel struts under cyclic load reversal", Rep. No. UCB/EERC-80/40; Earthquake Engineering Research Center, Univ. of California, Berkeley, CA, USA.

Black, C.J., Makris, N. and Aiken, I.D. (2004), "Component testing, seismic evaluation and characterization of buckling-restrained braces", *ASCE J. Struct. Eng.*, **130**(6), 880-894.

Celik, O.C., Berman, J.W. and Bruneau, M. (2005), "Cyclic testing of braces laterally restrained by steel studs", *ASCE J. Struct. Eng.*, **131**(7), 1114-1124.

Chao, S.-H., Karki, N.B. and Sahoo, D.R. (2013), "Seismic behavior of steel buildings with hybrid braced frames", *ASCE J. Struct. Eng.*, **139**(6), 1019-1032.

Christopoulos, C., Tremblay, R., Kim, H.-J. and Lacerte, M. (2008), "Self-centering energy dissipative bracing system for the seismic resistance of structure: Development and validation", *ASCE J. Struct. Eng.*, **134**(1), 96-107.

Coffin, L.F. and Tavernelli, J.F. (1962), "Experimental support for generalized equation predicting low cycle fatigue", *J. Basic Eng.*, **84**, 533-537.

CSI (2013), PERFORM-3D user guide; Computers and Structures Inc., Berkeley, CA, USA.

Erochko, J., Christopoulos, C., Tremblay, R. and Choi, H. (2011), "Residual drift response of SMRFs and BRB frames in steel buildings designed according to ASCE 7-05", *ASCE J. Struct. Eng.*, **137**(5), 589-599.

Fahnestock, L.A., Sause, R. and Ricles, J.M. (2007), "Seismic response and performance of buckling-restrained braced frames", *ASCE J. Struct. Eng.*, **133**(9), 1195-1204.

Fell, B.V., Kanvinde, A.M., Deierlein, G.G. and Myers, A.T. (2009), "Experimental investigation of inelastic cyclic buckling and fracture of steel braces", *ASCE J. Struct. Eng.*, **135**(1), 19-32.

FEMA 356 (2000), Pre-standard and commentary for the seismic rehabilitation of buildings; Federal Emergency Management Agency, Washington, DC, USA.

FEMA 450 (2003), NEHRP recommended provisions for seismic regulations for new buildings and other Structures; Part 1-Provisions, Federal Emergency Management Agency, Washington, DC, USA.

Fisher, J., Kulak, G. and Smith, I. (1997), "A fatigue primer for structural engineers", *Advance Technologies for Structural Systems*, Lehigh University; Bethlehem, PA, USA.

Ghowsi, A.F. and Sahoo, D.R. (2013), "Seismic performance of buckling-restrained braced frames with varying beam-column connections", *Int. J. Steel Struct.*, **13**(4), 607-621.

Ghowsi, A.F. and Sahoo, D.R. (2015), "Fragility assessment of buckling-restrained braced frames under near-field earthquakes", *Steel and Compos. Struct., Int. J.*, **19**(1), 173-190.

Hoveidae, N., Tremblay, R., Rafezy, B. and Davaran, A. (2015), "Numerical investigation of seismic behavior of short-core all-steel buckling restrained braces", *J. Constr.l Steel Res.*, **113**, 89-99.

Kiggins, S. and Uang, C.-M. (2006), "Reducing residual drift of buckling restrained braced frames as a dual system", *Eng. Struct.*, **28**(11), 1525-1532.

Kumar, P.C.A., Sahoo, D.R. and Kumar, N. (2015), "Limiting values of slenderness ratio for circular braces of concentrically braced frames", *J. Constr. Steel Res.*, **115**, 223-235.

Merritt, S., Uang, C.M. and Benzoni, G. (2003), "Sub-assemblage testing of star seismic buckling-restrained braces", Rep. TR-2003/04; Dept. of Structural Engineering, Univ. of California, La Jolla, CA, USA.

Mirtaheri, M., Geidi, A., Zandi, A.P., Alanjari, P. and Samani, H.R. (2011), "Experimental optimization studies on steel core lengths in buckling restrained braces", *J. Constr. Steel Res.*, **67**(8), 1244-1253.

Palmer, K.D., Christopulos, A.S., Lehman, D.E. and Roeder, C.W. (2014), "Experimental evaluation of cyclically loaded, large-scale, planar and 3-D buckling restrained braced frames", *J. Constr. Steel Res.*, **101**, 415-425.

Pandikkadavath, M.S. and Sahoo, D.R. (2016a), "Experimental study on reduced-length buckling restrained braces under slow cyclic loading", *Earthq. Struct.*, **10**(3), 699-716.

Pandikkadavath, M.S. and Sahoo, D.R. (2016b), "Analytical investigation on cyclic performance of buckling restrained braces with short yielding core segments", *Int. J. Steel Struct.*, **16**(4), 1273-1285.

Priestley, M.J.N. (2003), "Myths and fallacies in earthquake engineering, revisited", *Proceedings of the 9th Mallet Milne Lecture*, IUSS Press, Pavia, Italy, May.

Razavi, S.A., Mirghaderi, S.R., Hosseini, A. and Shemshadian, M.E. (2012), "Reduced length buckling restrained brace with steel plates as restraining segment", *Proceedings of the 13th World Conference on Earthquake Engineering*, Lisbon, Portugal, September.

Sabelli, R., Mahin, S.A. and Chang, C. (2003), "Seismic demands on steel braced frame buildings with buckling-restrained braces", *Eng. Struct.*, **25**(5), 655-666.

Sahoo, D.R. and Chao, S.-H. (2010), "Performance based plastic design method for buckling-restrained braces", *Eng. Struct.*, **32**(9), 2950-2958.

Sahoo, D.R. and Chao, S.-H. (2015), "Stiffness-based design for mitigation of residual displacements of buckling-restrained braced frames", *ASCE J. Struct. Eng.*, **149**(9), 04014229-1-04014229-13.

Somerville, P.G., Smith, M., Punyamurthala, S. and Sun, J. (1997), "Development of ground motion time histories for phase 2 of the FEMA/SAC steel project", FEMA/SAC, Rep. No. SAC/BD-97/04; Sacramento, CA, USA.

Tang, X. and Goel, S.C. (1988), "A fracture criterion for tubular bracing members and its application to inelastic dynamic analysis of braced steel structures", *Proceedings of the 9th World Conference on Earthquqke Engineering*, Vol. IV, Tokyo, Japan, August, pp. 285-290.

Tremblay, R., Archambault, M.H. and Filiatrault, A. (2003), "Seismic performance of concentrically braced steel frames made with rectangular hollow bracing members", *ASCE J. Struct. Eng.*, **129**(12), 1626-1636.

Tremblay, R., Bolduc, P., Neville, R. and Devall, R. (2006), "Seismic testing and performance of buckling-restrained bracing systems", *Can. J. Civil Eng.*, **33**(2), 183-198.

Tremblay, R., Lacerte, M. and Christopoulos, C. (2008), "Seismic response of multistory buildings with self-centering energy dissipative steel braces", *ASCE J. Struct. Eng.*, **134**(1), 108-120.

Tsai, K.C. and Hsiao, P.C. (2008), "Pseudo-dynamic test of a full-scale CFT/BRB frame-part II: Seismic performance of buckling-restrained braces and connection", *Earthq. Eng. Struct. Dyn.*, **37**(7), 1099-1115.

Tsai, K.C., Hsiao, B.C., Lai, J.W., Chen, C.H., Lin, M.L. and Weng, Y.T. (2003), "Pseudo dynamic experimental response of a full scale CFT/BRB composite frame", *Proceedings of Joint National Center for Research on Earthquake Engineering* (*NCREE*)/*Joint Research Center* (*JRC*) *Workshop on International Collaboration on Earthquake Disaster Mitigation Research*, NCREE, Taiwan, October.

Uriz, P. (2005), "Towards earthquake resistant design of concentrically braced steel structures", Ph.D. Dissertation; Department of Civil and Environmental Engineering, University of California, Berkeley, CA.

Usami, T., Kasai, A. and Kato, M. (2003), "Behavior of buckling-restrained brace members", *Proceedings of the 4th International Conference on Behavior of Steel Structures in Seismic Areas* (*STESSA*), Naples, Italy, June, pp. 211-216.

Usami, T., Wang, C. and Funayama, J. (2011), "Low cycle fatigue tests of a type of buckling restrained braces", *Procedia Engineering*, **14**, 956-964.

Watanabe, A., Hitomi, Y., Saeki, E., Wada, A. and Fujimoto, M. (1988), "Properties of brace encased in buckling-restrained concrete and steel tube", *Proceedings of the 9th World Conference on Earthquakes and Engineering*, Tokyo, Japan, August.

Wigle, V.R. and Fahnestock, L.A. (2010), "Buckling-restrained braced frame connection performance", *J. Constr. Steel Res.*, **66**(1), 65-74.

Wu, A.C., Lin, P.C. and Tsai, K.C. (2014), "High-mode buckling responses of buckling-restrained brace core plates", *Earthq. Eng. Struct. Dyn.*, **43**(3), 375-393.

CC